PPARγ agonists do not directly enhance basal or insulin-stimulated Na transport via the epithelial Na channel

6 authors, including:

Charity Nofziger
Paracelsus Medical University Salzburg
62 PUBLICATIONS **707** CITATIONS

SEE PROFILE

Lihong Chen
130 PUBLICATIONS **6,622** CITATIONS

SEE PROFILE

Chari Smith
Princeton University
32 PUBLICATIONS **837** CITATIONS

SEE PROFILE

Some of the authors of this publication are also working on these related projects:

Pharmacogenetics View project

EPITHELIAL TRANSPORT

Charity Nofziger · Lihong Chen · Michael Anne Shane
Chari D. Smith · Kathleen K. Brown
Bonnie L. Blazer-Yost

PPARγ agonists do not directly enhance basal or insulin-stimulated Na$^+$ transport via the epithelial Na$^+$ channel

Abstract Selective agonists of peroxisome proliferator-activated receptor gamma (PPARγ) are anti-diabetic drugs that enhance cellular responsiveness to insulin. However, in some patients, fluid retention, plasma volume expansion, and edema have been observed. It is well established that insulin regulates Na$^+$ reabsorption via the epithelial sodium channel (ENaC) located in the distal tubule. Therefore, we hypothesized that these agonists may positively modulate insulin-stimulated ENaC activity leading to increased Na$^+$ reabsorption and fluid retention. Using electrophysiological techniques, dose–response curves for insulin-mediated Na$^+$ transport in the A6, M-1, and mpkCCD$_{cl4}$ cell lines were performed. Each line demonstrated hormone efficacy within physiological concentration ranges and, therefore, can be used to monitor clinically relevant effects of pharmacological agents which may affect electrolyte transport. Immunodetection and quantitative PCR analyses showed that each cell line expresses viable and functional PPARγ receptors. Despite this finding, two PPARγ agonists, pioglitazone and GW7845 did not directly enhance basal or insulin-stimulated Na$^+$ flux via ENaC, as shown by electrophysiological methodologies. These studies provide important results, which eliminate insulin-mediated ENaC activation as a candidate mechanism underlying the fluid retention observed with PPARγ agonist use.

C. Nofziger · M. A. Shane · B. L. Blazer-Yost (✉)
Department of Biology, Indiana University
Purdue University at Indianapolis,
Indianapolis, IN, 46202
E-mail: bblazer@iupui.edu
Tel.: +1-317-2742846
Fax: +1-317-2781145

L. Chen · C. D. Smith · K. K. Brown
Division of Metabolic Disease, GlaxoSmithKline
Research and Development, Research Triangle Park,
NC 27709, USA

Introduction

There is an ever-increasing need for well-defined in vitro model systems which can be used to investigate intracellular signaling mechanisms within specific cell types of organ systems. The kidney exemplifies a complex organ in which the epithelial cells lining the tubules show segment-specific differences in transepithelial resistance and permeability as well as expression of distinct hormone receptors and transport proteins.

Cultured cell models expressing the in vivo characteristics of various tubular segments have been developed and serve as valuable models for studies that would not be possible in the context of the variability present in the whole organ. In the cortical collecting duct, the principal cells are responsive to three different hormones: aldosterone, antidiuretic hormone (ADH), and insulin/IGF1 (insulin-like growth factor 1). Each of these hormones positively regulates the epithelial Na$^+$ channel (ENaC), and, therefore, plays a crucial role in overall salt and water homeostasis.

While the pharmacology of the aldosterone response is relatively well defined in the available principal cell culture models, the responses to insulin are less well characterized. There is an emerging appreciation for the potential role of insulin in the development of hypertension in hyperinsulinemic states, thereby underscoring the need for well-characterized cell lines that can be used to model these clinical observations. Such cultured lines can also be utilized to investigate the efficacy and mechanism of action of pharmaceutical agents that target insulin-stimulated pathways.

Peroxisome proliferator-activated receptor gamma (PPARγ) is a nuclear transcription factor that, when activated, plays a functional role in free fatty acid metabolism and adipocyte differentiation [35]. The

thiazolidinedione (TZD) class of therapeutic compounds are high-affinity ligands for PPARγ [22], which have been shown to enhance cellular responsiveness to insulin, increase insulin-dependent glucose disposal, and improve hepatic sensitivity to insulin with overall durable improvement in glucose homeostasis. There are two FDA-approved TZDs—rosiglitazone (Avandia) and pioglitazone (Actos)—used in the treatment of type 2 diabetes mellitus (T2DM) either alone or in combination with metformin, sulfonylureas or insulin.

When used as monotherapy, there are reports of TZDs causing fluid retention that can result in plasma volume expansion and, in some patients, overt edema. The incidence of edema is increased when either of these agents is used in combination with insulin [27]. However, the mechanisms involved in the fluid retentive effects have not been well described. Interestingly, while the agents cause fluid retention, they also exhibit blood pressure lowering activity in normotensive and hypertensive rodents and humans [5, 6, 21, 32].

One potential target tissue for the fluid retentive action of these ligand-activated transcription factors is the vasculature. PPARγ is expressed in endothelial and smooth muscle cells [7, 21] and receptor activation appears to have direct vasodilatory effects in humans and rodents [5, 15, 28]. Even with changes in the vasculature, the observed clinical symptoms of salt and water retention suggest a primary or secondary effect on renal salt and water homeostasis. Localization of PPARγ in the glomerular mesangial cells [16, 18, 20] and the distal portions of the nephron [16, 19, 36] suggest a potential for direct effects of PPARγ agonists on renal function.

The current studies were designed to characterize the dose–response relationships for insulin-stimulated Na^+ transport in several principal cell culture models including the A6 (derived from *Xenopus laevis*) [3] and murine M-1 [33] and mouse principal kidney cortical collecting duct (mpkCCD$_{cl4}$) [2] cell lines. Subsequently, the cell lines were used to examine the potential renal involvement of PPARγ agonist-induced edema formation and to determine whether insulin's exacerbation of this effect could be manifested via Na^+ retention.

Materials and methods

Drugs and cell lines

The A6 and M-1 cell lines were obtained from ATCC (Rockville, MD, USA). The mpkCCD$_{cl4}$ cell line was provided by Dr. Alain Vandewalle (INSERM U478, Paris, France). Porcine insulin was obtained from Eli Lilly Corporation (Indianapolis, IN, USA). Amiloride was purchased from Sigma Chemical Co. (St. Louis, MO, USA). Pioglitazone and GW7845 were provided by GlaxoSmithKline (Research Triangle Park, NC, USA).

Cell culture

The A6 cell line was grown at 27°C in a humidified incubator gassed with 4.5% CO_2. Culture media consisted of seven parts Coon's F12 High Zinc and three parts Leibovitz's L15 (Irvine Scientific; Santa Ana, CA, USA), supplemented with 10% calf serum (ICN Biochemicals Inc., Irvine, CA, USA), 25 mM $NaHCO_3$, 25 U/ml penicillin, 25 mg/ml streptomycin, 1 mM Glutamax (Invitrogen; Carlsbad, CA, USA), and 12 mg/l ciprofloxacin (Voigt Global Distribution; Kansas City, MO, USA). The mammalian cell lines (M-1 and mpkCCD$_{cl4}$) were grown at 37°C in a humidified incubator gassed with 5% CO_2. Culture media consisted of DMEM/F12 base media (Invitrogen) supplemented with 5% fetal bovine serum (ICN Biochemicals Inc.), 1 mM Glutamax, 25 U/ml penicillin, 25 mg/ml streptomycin, and 12 mg/l ciprofloxacin. For all cell lines, media was replaced every 2 days. Cell cultures were maintained in plastic flasks until confluent and subcultured at a 1 : 10 dilution. For electrophysiological experiments, cells were subcultured onto permeable supports (Costar Transwells; Fisher, Chicago, IL, USA) at confluent density. All cells were grown on permeable supports for at least 14 days prior to electrophysiological studies.

Electrophysiology

Transwell filters containing confluent cell monolayers were clamped in a Ussing chamber and connected to a voltage clamp apparatus (WPI; Sarasota, FL, USA) via current and voltage electrodes. The initial transepithelial voltage was clamped to zero and the resulting short-circuit current (SCC) measured. The cells were bathed with the appropriate serum-free media, which was maintained at either 27 or 37°C for the A6 cell line and mammalian cell lines, respectively. A 5/95% CO_2/O_2 gas lift served to circulate the bathing media, as well as maintain pH. All cell lines were serum-starved for 18–24 h prior to electrophysiological studies. Either pioglitazone (10 μM) or GW7845 (100 nM) was added to the serosal bathing media 18–24 h prior to and during electrophysiological studies. In all experiments, insulin was added to the serosal bathing media and amiloride (10^{-5} M) was added to the apical bathing media 30 min after insulin addition. Transepithelial resistance (an indication of cellular viability) was monitored throughout the entire duration of each electrophysiological experiment by pulsing the tissues with a 2,000 μV pulse every 200 s. Resistance values were calculated from the resulting current deflections using Ohm's law. By convention, an increase in SCC is indicative of cation absorption (apical to basal flux) or of anion secretion (basal to apical flux). A6 and mpkCCD$_{cl4}$ cells were only used in statistical analyses if tissue resistances were ≥1,000 $\Omega \cdot cm^2$. M-1 cells were only included in statistical analyses if tissue resistances were ≥500 $\Omega \cdot cm^2$.

Total RNA extraction, reverse transcription, and quantitative polymerase-chain reaction

Total RNA from untreated M-1 and mpkCCD$_{cl4}$ cells grown on plastic (for PPARγ gene expression analyses) or from PPARγ-treated mpkCCD$_{cl4}$ cells grown on semi-permeable supports (for CD36 and SGK gene expression analyses) were extracted using RNeasy mini column (Qiagen; Valencia, CA, USA) and digested with DNase (Qiagen) following the manufacturer's instructions to remove DNA contamination. One microgram of cleaned total RNA was reverse transcribed in 100 µl reaction using the High Capacity cDNA Archive Kit (Applied Biosystems; Foster City, CA, USA). Quantitative polymerase-chain reaction (qPCR) was performed and analyzed using ABI PRISM 7000 Sequence Detection System (Applied Biosystems) with gene-specific primers and probes. Mouse-specific oligonucleotides used in qPCR analyses are outlined in Table 1.

Gel electrophoresis and western blotting

Cells grown on permeable supports were washed in ice-cold serum-free culture media and solubilized with lysis buffer (4% SDS, 10% glycerol, and 1 mM DTT in 0.05 M Tris, pH 6.8). Lysates were sonicated for 20 1-s pulses with a titanium-tip sonicator (20% duty cycle, Branson Sonifier 450). Protein concentration was determined using the DC protein assay kit (Biorad; Hercules, CA, USA). The cell lysates were separated by SDS-PAGE on 7.5% acrylamide gels and blotted onto Immobilon-P transfer membrane (Millipore Corp.; Bedford, MA, USA). The membranes were blocked with 5% milk-TBS, pH 7.5 and subsequently incubated overnight at 4°C with gentle agitation with either an anti-PPARγ antibody (Affinity BioReagents; Golden, CO) at a 1:3,000 dilution, an anti-CD36 antibody (Cayman Chemical; Ann Arbor, MI) at a 1:1,000 dilution, or an anti-SGK antibody (Dr. Nicola Perrotti; Univ. Magna Graecia of Catanzaro, Catanzaro, Italy) at a 1:1,000 dilution followed by incubation with anti-rabbit antibody conjugated to horseradish peroxidase (Upstate Inc.; Charlottesville, VA, USA) at a 1:10,000 or 1:60,000 dilution. Both antibodies were diluted in 0.5% milk-TBS, pH 7.5. The protein bands were visualized with SuperSignal West Dura enhanced chemiluminescence reagent (Pierce; Rockford, IL, USA) and developed on film.
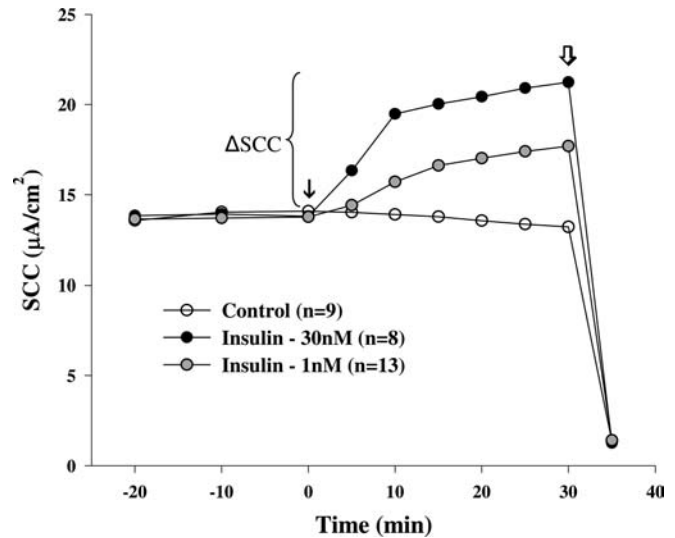

Fig. 1 Insulin-stimulated Na$^+$ reabsorption in A6 cells. Confluent cultures were serum-starved 18–24 h. The *solid arrow* indicates time of insulin addition. The *open arrow* indicates time of amiloride (10^{-5} M) addition. Varying insulin concentrations result in concomitant rises in net SCC. The magnitude (Δ SCC) of reabsorptive Na$^+$ flux stimulated by 30 nM insulin is indicated by the bracket (SCC$_{t = 30\ min}$−SCC$_{t = 0\ min}$). Symbols represent the mean of n experiments. The standard error bars were not included for clarity. Significance of the responses are shown in Fig. 2

Statistical analyses

Symbols and/or bar graphs are represented as means ± standard error of the mean (SEM). Differences between groups were evaluated using Student's t-test. The p values are defined in the figure legends.

Results

In cultured cells, electrogenic transport such as trans-epithelial Na$^+$ flux can be measured by clamping the spontaneous potential difference of a confluent, high-resistance monolayer to zero and recording the SCC. Ion transport generated by Na$^+$ flux in the reabsorptive direction can be quantitated with the use of an ENaC-specific inhibitor, amiloride. Representative ion transport responses of the A6 cell line to maximal and sub-maximal concentrations of insulin are shown in Fig. 1. In this cell line, both basal (control) and insulin-stimulated ion flux are predominantly amiloride-sensitive. The ion transport traces of the M-1 and mpkCCD$_{cl4}$ cells are similar to that seen in the A6 cells, except that the M-1

Table 1 Primer sets and probes: oligonucleotides used for qPCR analyses

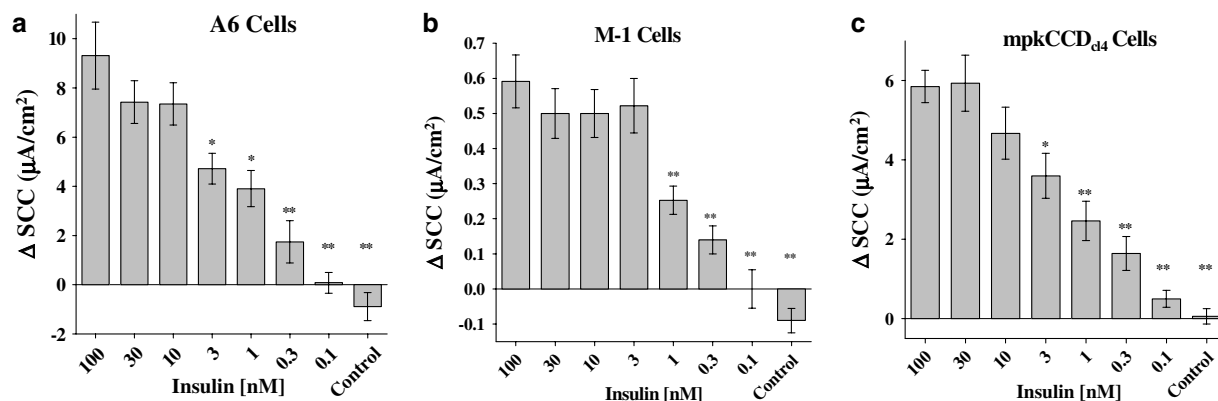| Gene	Forward primer	Reverse primer	Probe
PPARγ	tgaataaagatggagtcctcatctca	ggcttccgcaggtttttga	agggccaaggattcatgaccaggg
CD36	cctgcagaaatactagccaacacc	tgagtccatgcagtttcc	cgaaaacgctggcttctgtatacccga
SGK	cggtggactggtggtgtctt	agccgtgttccggctataaa	ctgtcctgtatgagatgctctacggcctg

Fig. 2 Insulin dose–response curves in principal cell culture models. (**a**) A6, (**b**) M-1, and (**c**) mpkCCD$_{cl4}$ cells were serum-starved 18–24 h and subsequently stimulated with varying concentrations of insulin. The magnitude of insulin-stimulated Na$^+$ flux is depicted in *bar graphs* representing means ± SEM and are measured as ($\Delta SCC = SCC_{t=30\ min} - SCC_{t=0\ min}$) in the case of A6 and mpkCCD$_{cl4}$ cells, and as ($\Delta SCC = SCC_{t=10\ min} - SCC_{t=0\ min}$) for the M-1 cells. The number of experiments for each insulin dose are between 5 and 13, 5 and 14, and 5 and 11 for the A6, M-1, and mpkCCD$_{cl4}$ cells, respectively. Statistical significance compared to the maximal insulin dose (30 nM) is denoted using Student's *t*-test; * $p \leq 0.05$, ** $p \leq 0.01$

cells display a lower rate of basal ion transport as compared to the other two cell lines (data not shown).

The dose–response relationships between Na$^+$ flux and insulin concentrations for all three cell lines are expressed as the insulin-stimulated increase over baseline (Δ SCC) in Fig. 2. Under these experimental conditions, the rise in SCC elicited by 30 nM insulin is maximal in all cell lines. The dose–response curves elicited in the amphibian and mammalian cell lines are virtually identical. However, in the M-1 cells, the magnitude of the insulin-stimulated changes in net transport are approximately tenfold less than that observed in either the A6 or mpkCCD$_{cl4}$ cells (compare the SCC scales between the panels in Fig. 2). The rate of basal transport observed in the M-1 cell line was also proportionally lower. Each cell line exhibits a dose-responsive relationship of insulin-stimulated Na$^+$ transport within normal rodent plasma insulin concentrations (Table 2).

We performed qPCR on RNA isolated from confluent M-1 and mpkCCD$_{cl4}$ cells and measured basal amounts of PPARγ mRNA expression. Both cell lines express similar amounts of PPARγ transcript in the basal state (Fig. 3a). Concurrently, a band corresponding to PPARγ protein was detected in the A6, M-1, and mpkCCD$_{cl4}$ cell lines (Fig. 3b). The M-1 cells express a higher level of PPARγ protein as compared to the mpkCCD$_{cl4}$ cells.

In order to verify that the agonists used in these studies were, in fact, functional, PPARγ-induced gene expression was determined using the mpkCCD$_{cl4}$ cells. CD36 is a protein commonly upregulated by PPARγ in multiple tissues [25]. Long-term (18–24 h) incubation with either pioglitazone or GW7845 induced a significant increase in CD36 mRNA (Fig. 4a). Concurrently, CD36 protein abundance was induced upon treatment with either of the two agonists (Fig. 4b). The effect of the two agonists on expression of serum and glucocorticoid induced kinase (SGK)—an enzyme that was previously reported to be upregulated with PPARγ agonist treatment [19]—was also investigated in the mpkCCD$_{cl4}$ cells (Fig. 4). We did not observe any changes in the levels of SGK transcript or protein expression after a long-term (18–24 h) incubation with either PPARγ agonist.

The majority of basal ion transport in each cell line is amiloride-sensitive, indicating that it is predominantly due to reabsorptive Na$^+$ movement via ENaC. It is possible that the PPARγ agonists may affect salt and water homeostasis by modulating basal ENaC activity rather than by regulating hormonally induced changes in channel transport. However, differences in the amount of basal Na$^+$ transport were not observed in either the A6 or the mpkCCD$_{cl4}$ cell lines after long-term (18–24 h) pioglitazone or GW7845 treatment. The effect of short-term (2 h) agonist incubation was examined in the mpkCCD$_{cl4}$ cell line. Neither agonist affected basal Na$^+$ transport after 2 h (data not shown). On the other hand, long-term treatment with GW7845 significantly decreased basal ion transport compared to the untreated tissue in the M-1 cell line (Fig. 5). The explanation for the anomalous GW7845-mediated decrease in basal ion flux in the M-1 cell line and not the other two cell lines has not yet been determined.

To ascertain potential insulin-sensitizing effects of the PPARγ agonists, a submaximal (1 nM) insulin concentration was used to stimulate cells preincubated

Table 2 Rat insulin concentrations

|	Fasted	Nonfasted
Control	0.26 nM [34]	0.36 nM [34]
Fructose-fed (hyperinsulinemic)	0.71 nM [34]	1.41 nM [34]
Control	0.26 nM [14]	
Insulin infusion (hyperinsulinemic)	0.71 nM [14]	

Values represent insulin concentrations in rats during control and hyperinsulinemic situations.

Fig. 3 Basal PPARγ expression levels in M-1 and mpkCCD$_{cl4}$ cells. (**a**) The expression of PPARγ mRNA in M-1 and mpkCCD$_{cl4}$ cells was normalized to the expression of β-actin mRNA and presented as arbitrary units. (**b**) PPARγ protein expression in A6, M-1, and mpkCCD$_{cl4}$ cells. Confluent monolayers of each cell line were lysed, separated by SDS-PAGE, blotted onto transfer membrane, and probed for PPARγ. Equal amounts of protein (100 μg) was loaded in each lane. The *arrow* shows an ~47 kDa protein corresponding to PPARγ. Results are representative of three independent experiments
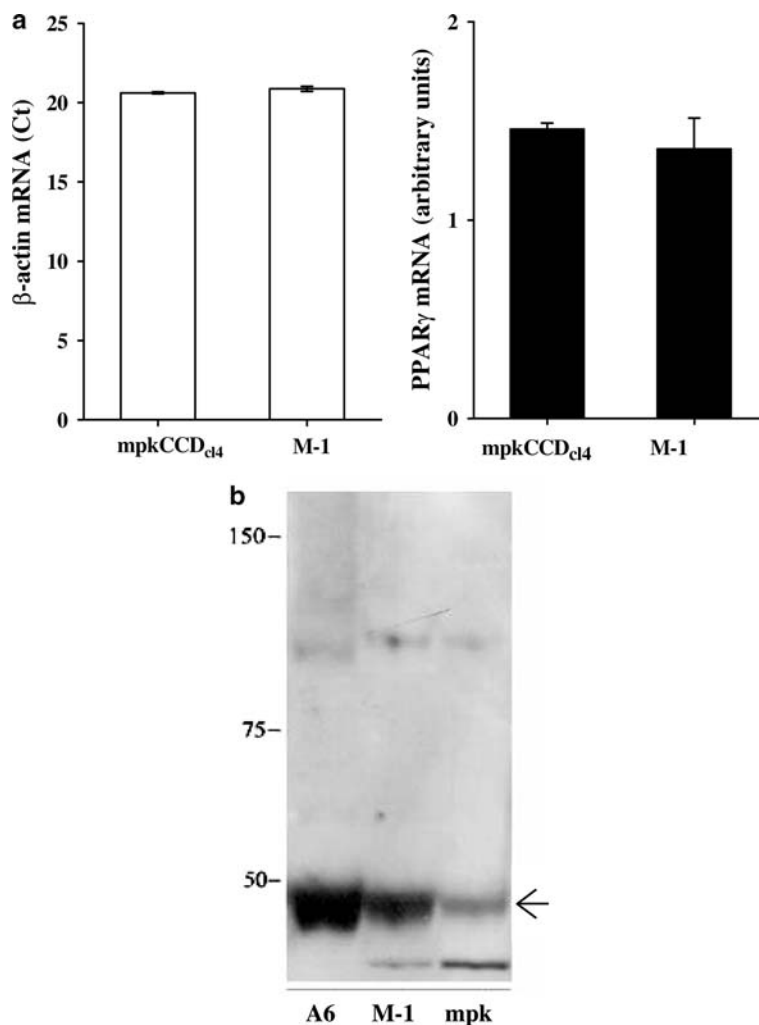
(18–24 h) in the presence or absence of either agonist. Neither pioglitazone nor GW7845 treatment significantly increased the amount of Na$^+$ flux elicited by a submaximal (1 nM) insulin dose in any of the three cell lines (Fig. 6).

Discussion

Monogenetic aberrations in proteins belonging to the hormonal axes that regulate ENaC activity have been shown to cause changes in salt and fluid balance leading to hypertensive or hypotensive states [9, 31]. Insulin enhances Na$^+$ reabsorption in the distal tubule and, in humans, there is a correlation between insulin resistance, hyperinsulinemia and hypertension that is independent of age, gender, or degree of obesity [8, 11, 12, 24, 29, 30]. The in vivo studies have been substantiated by work in cell culture models where it has been conclusively shown that insulin regulates ENaC activity and cell surface expression [1, 3, 4].

We focused our study on the potential for direct effects of PPARγ activation in the regulation of salt and water balance in the principal cells of the distal tubule. Interestingly, like insulin-mediated insertion of GLUT-4 transporters into the plasma membrane of adipose and skeletal muscle cells [10, 37], insulin-mediated insertion of ENaC into the apical membrane of principal cells is under the control of the phosphoinositide (PI) pathway [3, 4, 13]. Therefore, we postulated that PPARγ ligands may have actions not only on cellular glucose uptake but also on expression and cellular localization of proteins that regulate other transport processes such as ENaC-mediated Na$^+$ absorption. In addition, PPARγ is found in the distal tubule and it is conceivable that the volume expansion observed with agonist treatment may be linked to the natriferic effects of insulin or, alternatively, may be the result of a direct PPARγ effect on Na$^+$ transport.

The significant findings from this investigation include: (1) net ENaC-mediated Na$^+$ flux in three distinct in vitro models of the renal principal cell type exhibit similar dose-dependent regulation by insulin; (2) the three cell lines express functional PPARγ and are, therefore, capable of modulation by PPARγ-activating agents; and (3) activation of PPARγ with either pioglitazone (a true TZD) or the more potent PPARγ ago-
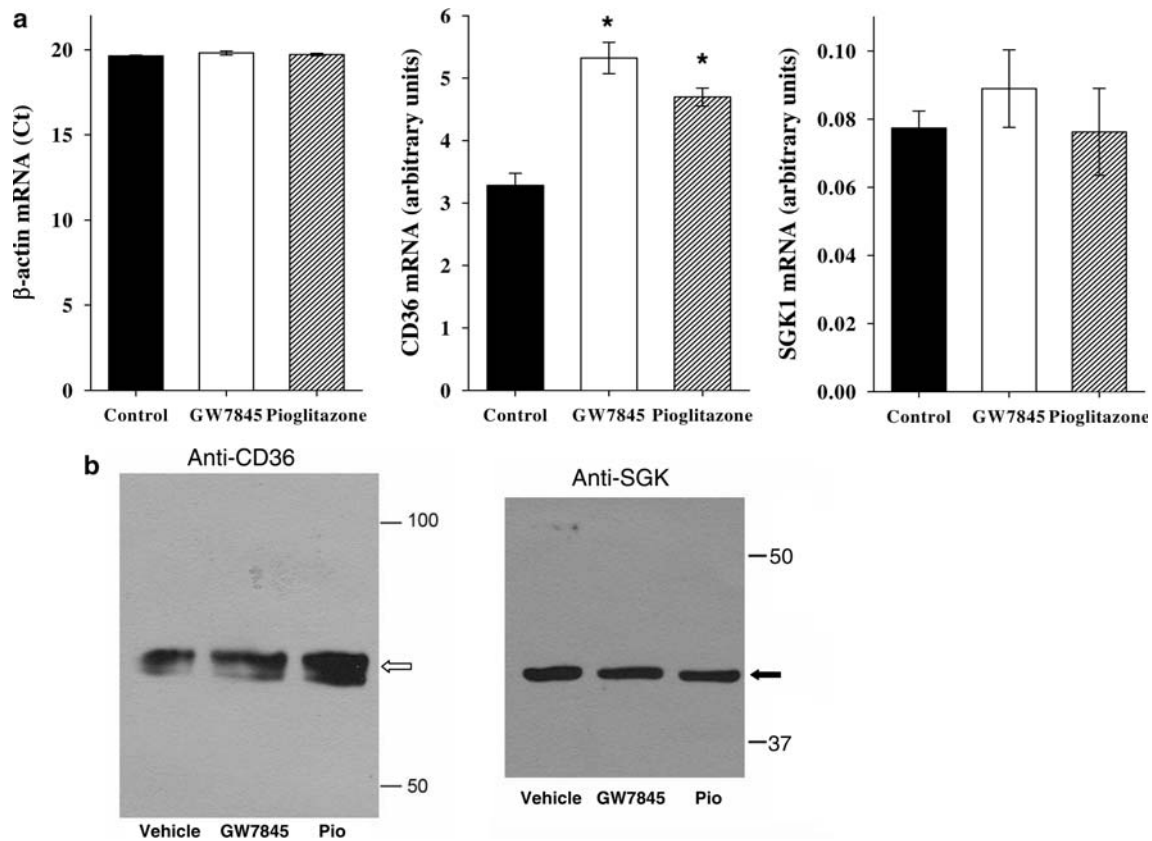
Fig. 4 Effect of PPARγ agonists on CD36 and SGK expression. Confluent monolayers of mpkCCD$_{cl4}$ cells were serum-starved overnight and treated with either vehicle (*black bars*), 100 nM GW7845 (*white bars*), or 10 μM pioglitazone (*hashed bars*) 18–24 h. (**a**) CD36 mRNA or SGK mRNA was normalized to the expression of β-actin mRNA and presented as arbitrary units. *Bars* represent means ± SEM. Statistical significance in gene expression between PPARγ-treated tissues and vehicle-treated tissues for CD36 mRNA is denoted using Student's *t*-test; * $p \leq 0.05$. Results are representative of two independent experiments. (**b**) Whole cell lysates of serum-starved mpkCCD$_{cl4}$ cells treated 18–24 h with either vehicle (DMSO), pioglitazone (10 μM), or GW7845 (100 nM) were separated by SDS-PAGE, blotted onto transfer membrane, and probed for CD36 or SGK. Equal amounts of protein (100 μg) was loaded in each lane. The *open arrow* shows a doublet migrating at ∼80 kDa corresponding to CD36, whereas the *solid arrow* shows a band migrating at ∼46 kDa corresponding to SGK. Results are representative of two individual experiments

nist, GW7845 (a non-TZD), did not change the magnitude of (a) basal Na$^+$ transport in two of the cell lines (A6 and mpkCCD$_{cl4}$) or (b) insulin-stimulated Na$^+$ transport in any of the cell lines.

There is a striking similarity between the cell lines with respect to the insulin dose–response curves for activation of Na$^+$ transport. These studies represent the first demonstration of insulin dose–response relationships for the murine cell lines (M-1 and mpkCCD$_{cl4}$). The insulin concentration eliciting an approximately half-maximal response (0.3 nM) in each cell line is within normal insulin levels for both the fasted and non-fasted states in rats (compare Table 2 with Fig. 2), demonstrating that the insulin dose–response relationship in these murine cell lines shows efficacy in the physiological range. The same is true for the A6 cell line.

The discrepancy between the net magnitude of insulin-stimulated Na$^+$ flux in the A6, M-1, and mpkCCD$_{cl4}$ cells remains elusive; but it should be noted that these differences are not unique to insulin. The magnitude of the natriferic responses elicited by aldosterone and ADH vary considerably from one cell line to another but, in general, follow the same trend observed in the insulin studies. The explanation may lie in the amount and/or activity of ENaCs, or, alternatively, may be dictated by the amount of ENaC regulatory components that each line expresses.

Previous studies utilizing tissue from dissected nephrons have found PPARγ expression in various segments of the distal tubule. In situ hybridization has shown the expression of PPARγ transcripts in human, rabbit, and rat collecting duct (CD) [17, 19, 36]. Immunohisto-chemical studies have indicated the presence of the PPARγ protein in freshly isolated rabbit inner medullary collecting duct (IMDC) and in primary cultures of IMCD as well as CCDs [17]. Recently, Hong et al. used immunohistochemical staining to show the expression of PPARγ protein in the distal convoluted tubule, CCDs, and medullary CDs in human kidney sections. In addition, this group detected PPARγ transcripts in a mouse IMCD cell line (mIMCD-K2) as well as in M-1 and human CCD principal cell lines [19].

We detected transcripts for PPARγ in the mpkCCD$_{cl4}$ and M-1 cells. The A6 cell line was excluded

a

A6 Cells

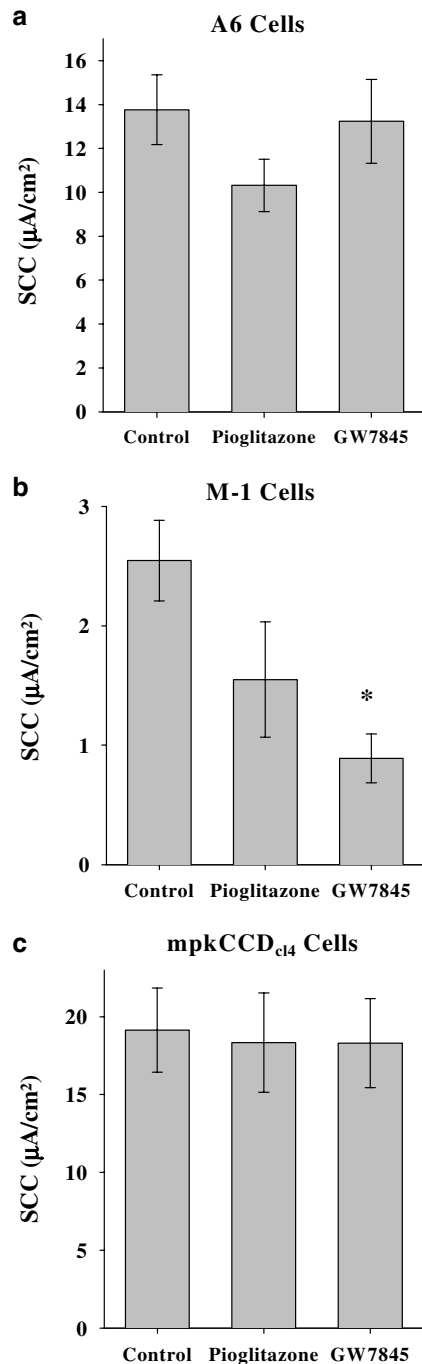
b

M-1 Cells

c

mpkCCD$_{cl4}$ Cells

Fig. 5 Effect of pioglitazone and GW7845 on basal ion transport. (a) A6 cells, (b) M-1 cells, and (c) mpkCCD$_{cl4}$ cells were serum-starved overnight and treated with either pioglitazone (10 μM) or GW7845 (100 nM) 18–24 h. Basal transport rates just before addition of insulin (time = 0) in control, pioglitazone, or GW7845 treated cells were compared. *Bars* depict means ± SEM. The number of experiments for each condition (control or PPARγ-treated) range between 8 and 13, 4 and 11, and 9 and 11 for A6, M-1, and mpkCCD$_{cl4}$ cells, respectively. Statistical significance compared to the untreated cells is denoted using Student's *t*-test; *$p \leq 0.05$

from this analysis due to lack of species-specific primers. The results in the M-1 cell line substantiate the previous findings of Yang et al., while the results in the

mpkCCD$_{cl4}$ cell line are novel. Each cell line also expresses PPARγ protein in varying amounts. Interestingly, the PPARγ protein expression in the M-1 and mpkCCD$_{cl4}$ cells does not follow the same trend as the mRNA expression. This observation may explain the baseline-lowering effect of GW7845 in the M-1, but not mpkCCD$_{cl4}$ cell line (Fig. 3b, c). However, this reasoning is not consistent when considering the protein expression of PPARγ in the A6 cells. GW7845 did not cause a decline in basal transport in this line (Fig. 3a) even though the A6 cells express the highest amount of PPARγ protein.

We next explored the functionality of the PPARγ agonists used in these studies. qPCR was used to assess PPARγ-induced gene expression in the mpkCCD$_{cl4}$ cells. This line was chosen for the gene analyses due to the availability of species-specific primer sets, as well as the robust nature of their natriferic responses to insulin. CD36 is a transmembrane glycoprotein involved in foam cell formation and this protein has been shown to be upregulated in response to PPARγ treatment [25]. Pioglitazone and GW7845 both caused a significant increase in CD36 mRNA and protein expression, verifying the functionality of the PPARγ agonists.

In summary, PPARγ is present in the sections of the kidney containing principal cells as well as in cultured principal cell lines. It has been demonstrated that each cell line utilized in this study also expresses the protein and/or mRNA for each of the ENaC subunits [2, 23, 26]. Thus, the key components of the potential PPARγ-regulated pathway are expressed in the cell lines used.

Our studies suggest that the TZDs are not contributing to the fluid retention through direct regulation of ENaC or insulin-stimulated ENaC activity. It is possible that the agonists may be acting on water and Na$^+$ transporting machinery located prior to the distal convoluted tubule. Rosiglitazone treatment in Sprague–Dawley rats was shown to increase protein abundance of the sodium-hydrogen exchanger-3 (NHE3), the primary source of Na$^+$ reabsorption in the proximal tubule [32]. However, in the same study, expression of the collecting duct aquaporins 2 and 3 were shown to be up-regulated when challenged with rosiglitazone, suggesting that ADH may have a role in PPARγ-mediated fluid retention and, in agreement with the previously cited papers, indicate a distal site of action. Also consistent with a distal effect are the observations of Hong and colleagues, who showed that treatment of a PPARγ-expressing human CCD cell line with either rosiglitazone (2 μM) or pioglitazone (20 μM) increased the translocation of αENaC to the plasma membrane, although the functional ramifications of this observation were not explored [19].

In the Hong et al. study, the translocation of αE-NaC was accompanied by an upregulation of SGK mRNA and activity within 4 h of PPARγ agonist treatment. SGK is a downstream enzyme activated in the PI pathway—a signaling system shared by various
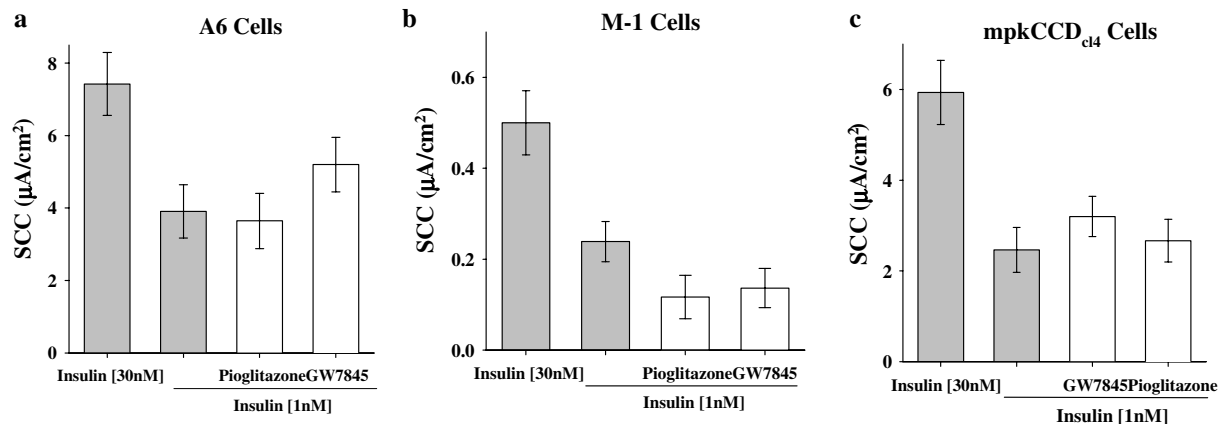
Fig. 6 Effect of PPARγ agonists on Na$^+$ transport stimulated by a submaximal (1 nM) insulin dose. Either pioglitazone (10 μM) or GW7845 (100 nM) was added to the serosal bathing media of confluent (**a**) A6, (**b**) M-1, or (**c**) mpkCCD$_{cl4}$ cells 18–24 h prior to and during the electrophysiological studies. The magnitude of Na$^+$ flux stimulated by a submaximal (1 nM) insulin dose is depicted in *bar graphs* representing means ± SEM and are measured as (Δ SCC = SCC$_{t = 30\ min}$ − SCC$_{t = 0\ min}$) in the case of A6 and mpkCCD$_{c14}$ cells, and as (Δ SCC = SCC$_{t = 10\ min}$ − SCC$_{t = 0\ min}$) for M-1 cells. The number of experiments for each experimental condition (insulin alone or insulin plus PPARγ agonist) range between 8 and 13, 5 and 14, and 9 and 11 for A6, M-1, and mpkCCD$_{cl4}$ cells, respectively. Statistical analyses indicated that neither pioglitazone nor GW7845 had a significant effect on the 1 nM insulin response in any of the cell lines

ENaC-regulating hormones. In functional studies, over-expression of wild-type SGK has been shown to increase basal, but not insulin-stimulated Na$^+$ transport through ENaC [13]. We did not observe PPARγ-induced changes in the amount of SGK transcript or expressed protein in the mpkCCD$_{cl4}$ cells. In addition, neither PPARγ agonist induced basal or insulin-stimulated ENaC activity in the same cell line. It is possible that the PPARγ agonists may regulate SGK activity by a post-translational mechanism. If this is the case, one would expect PPARγ agonist treatment to positively regulate basal ENaC activity; however in the mpkCCD$_{cl4}$ cells, we did not find significant increases in basal ENaC transport either 2 h (data not shown) or 18–24 h (Fig. 5) after treatment with GW7845 (100 nM) or pioglitazone (10 μM). The differences in the experimental results between the Hong et al. study and the present study may be explained by differences in the cell lines utilized and/or PPARγ agonist concentrations tested.

On the other hand, SGK has been implicated as both necessary and rate-limiting for ADH-stimulated Na$^+$ transport [13]. Therefore, it is entirely possible that the PPARγ agonists may be modulating ENaC and/or other transporter function via other hormonal pathways independent of insulin.

We have verified that three cell culture models of the principal cell type respond to physiologically relevant insulin concentrations in a dose-dependent manner. In addition, we have shown that PPARγ agonists do not potentiate insulin-mediated Na$^+$ flux in any of the lines, suggesting that PPARγ activation does not regulate fluid homeostasis via a direct effect on insulin-stimulated ENaC activity in isolated cell lines. The in vivo situation may be more complex, encompassing factors that are not found in cultured cells. These findings are important in ruling out targets for clinical intervention of the fluid retention and will provide the basis for future studies involving the regulation of other renal transporter functions by PPARγ.

References

1. Baxendale-Cox LM, Duncan RL (1999) Insulin increases sodium (Na$^+$) channel density in A6 epithelia: implications for expression of hypertension. Biol Res Nurs 1:20–29
2. Bens M, Vallet V, Cluzeaud F, Pascual-Letallec L, Kahn A, Rafestin-Oblin ME, Rossier BC, Vandewalle A (1999) Corticosteroid-dependent sodium transport in a novel immortalized mouse collecting duct principal cell line. J Am Soc Nephrol 10:923–934
3. Blazer-Yost BL, Esterman MA, Vlahos CJ (2003) Insulin-stimulated trafficking of ENaC in renal cells requires PI 3-kinase activity. Am J Physiol Cell Physiol 284:C1645–C1653
4. Blazer-Yost BL, Vahle JC, Byars JM, Bacallao R (2004) Real-time three dimensional imaging of lipid signal transduction: apical membrane insertion of epithelia Na$^+$ channels. Am J Physiol Cell Physiol 321(9):580–585
5. Buchanan TA, Meehan WP, Jeng YY, Yang D, Chan TM, Nadler JL, Scott S, Rude RK, Hsueh WA (1995) Blood pressure lowering by pioglitazone: evidence for a direct vascular effect. J Clin Invest 96:354–360
6. Callahan MF, Brown KK, Baer PG, Smith TL (2002) Effects of a PPARγ agonist GI262570, on cardiac output, arterial blood pressure, and systemic vascular resistance in conscious rats. Circulation 106:560
7. Calnek DS, Mazzella L, Roser S, Roman J, Hart CM (2003) Peroxisome proliferator-activated receptor gamma ligands increase release of nitric oxide from endothelial cells. Arterioscler Thromb Vasc Biol 23:53–57
8. Carretero OA, Oparil S (2000) Essential hypertension. Circulation 1001:429–453

9. Chang SS, Grunder S, Hanukoglu A, Rosler A, Mathew PM, Hanukoglu I, Schild L, Lu Y, Shimkets RA, Nelson-Williams C, Rossier BC, Lifton RP (1996) Mutations in subunits of the epithelial sodium channel cause salt wasting with hyperkalaemic acidosis, pseudohypoaldosteronism type I. Nat Genet 12:248–253

10. Cheatham B, Vlahos CJ, Cheatham L, Wang L, Blenis J, Kahn CR (1994) Phosphatidylinositol 3-kinase activation is required for insulin stimulation of pp70 S6 kinase, DNA synthesis, and glucose transporter translocation. Mol Cell Biol 14:4902–4911

11. DeFronzo RA (1981) The effect of insulin on renal sodium metabolism: a review with clinical implications. Diabetologia 21:165–171

12. DeFronzo RA, Cooke CR, Andres R, Faloona GR, Davis PJ (1975) The effect of insulin on renal handling of sodium, potassium, calcium, and phosphate in man. J Clin Invest 55:845–855

13. Faletti CJ, Perrotti N, Taylor SI, Blazer-Yost BL (2002) Sgk: an essential convergence point for peptide and steroid hormone regulation of ENaC-mediated Na^+ transport. Am J Physiol Cell Physiol 282:C494–C500

14. Fang T-C, Huang W-C (1998) Angiotensin receptor blockade blunts hyperinsulinemia-induced hypertension in rats. Hypertension 32:235–242

15. Gardiner SM, Nunez DJR, Baer PG, Brown KK, Bennett T (2004) Regional hemodynamic effects of the *n*-(2-benzoylphenyl)-l-tyrosine peroxisome proliferator-activated receptor-*γ* ligand GI262570, in conscious rats. J Pharm Exp Ther 310:1222–1233

16. Guan Y, Breyer MD (2001) Peroxisome proliferator-activated receptors (PPARs): novel therapeutic targets in renal disease. Kidney Int 60:14–30

17. Guan Y, Zhang Y, Davis L, Breyer MD (1997) Expression of peroxisome proliferator-activated receptors in urinary tract of rabbits and humans. Am J Physiol Renal Physiol 273:F1013–F1022

18. Guan Y, Zhang Y, Schneider A, Davis L, Breyer RM, Breyer MD (2001) Peroxisome proliferators-activated receptor-*γ* activity is associated with renal microvasculature. Am J Physiol Renal Physiol 281:F1036–F1046

19. Hong G, Lockhart A, Davis B, Rahmoune H, Baker S, Ye L, Thompson P, Shou Y, O'Shaughnessy K, Ronco P, Brown J (2003) PPAR*γ* activation enhances cell surface ENaC*α* via upregulation of SGK1 in human collecting duct cells. FASEB J 17:1966–1968

20. Hseuh WA, Nicholas SB (2002) Peroxisome proliferator-activated receptor-*γ* in the renal mesangium. Hypertension 11:191–195

21. Kotchen TA, Zhang HY, Reddy S (1996) Effect of pioglitazone on vascular reactivity in vivo and in vitro. Am J Physiol 270:R660–R666

22. Lehmann JM, Moore LB, Smith-Oliver TA, Wilkison WO, Willson TM, Kliewer SA (1995) An antidiabetic thiazolidinedione is a high affinity ligand for peroxisome proliferator-activated receptor gamma (PPARgamma). J Biol Chem 270:12953–12956

23. May A, Puoti, A, Gaeggeler H-P, Horisberger J-D, Rossier B (1997) Early effect of aldosterone on the rate of synthesis of the epithelial sodium channel α subunit in A6 renal cells. J Am Soc Nephrol 12:1813–1822

24. McFarlane SI, Banerji M, Sowers JR (2001) Insulin resistance and cardiovascular disease. J Clin Endocrin Metabol 86:713–718

25. Motojima K, Passilly PP, Peters JM, Gonzalez FJ, Latruffe N (1998) Expression of putative fatty acid transporter genes are regulated by peroxisome proliferator-activated receptor alpha and gamma activators in a tissue- and inducer-specific manner. J Biol Chem 273:16710–16714

26. Nakhoul NL, Hering-Smith KS, Gambala C, Hamm LL (1998) Regulation of sodium transport in M-1 cells. Am J Physiol 275:F998–F1007

27. Nesto RW, Bell D, Bonow RO, Fonseca V, Grundy SM, Horton ES, Le Winter M, Porte D, Semenkovich CF, Smith S, Young LH, Kahn R (2003) Thiazolidinedione use, fluid retention and congestive heart failure: a consensus statement from the American Heart Association and American Diabetes Association. Circulation 108:2941–2948

28. Parulkar AA, Pendergrass ML, Granda-Ayala R, Lee TR, Fonseca VA (2001) Nonhypoglycemic effects of thiazolidinediones. Ann Intern Med 134:61–71

29. Reaven GM (1999) Insulin resistance: a chicken that has come home to roost. Ann NY Acad Sci 892:45–57

30. Sharma AM, Schorr U, Distler A (1993) Insulin resistance in young, salt-sensitive normotensive subjects. Hypertension 21:273–279

31. Shimkets RA, Warnock DG, Bositis CM, Nelson-Williams C, Hansson JH, Schambelan M, Gill JR Jr, Ulick S, Milora RV, Findling JW et al (1994) Liddle's Syndrome: heritable human hypertension caused by mutations in the β subunit of the epithelial sodium channel. Cell 79:407–414

32. Song J, Knepper M, Hu X, Verbalis JG, Ecelbarger CA (2004) Rosiglitazone activates renal sodium- and water-reabsorptive pathways and lowers blood pressure in normal rats. J Pharmacol Exp Ther 308:426–433

33. Stoos BA, Naray-Fejes-Toth A, Carretero OA, Ito S, Fejes-Toth G (1991) Characterization of a mouse cortical collecting duct cell line. Kidney Int 39:1168–1175

34. Takagawa Y, Berger ME, Hori MT, Tuck ML, Golub MS (2001) Long-term fructose feeding impairs vascular relaxation in rat mesenteric arteries. Am J Hypertens 14:811–817

35. Willson TM, Lambert MH, Kliewer SA (2001) Peroxisome proliferator-activated receptor *γ* and metabolic disease. Annu Rev Biochem 70:341–367

36. Yang T, Michele DE, Park J, Smart AM, Lin Z, Brosius FC III, Schnermann JB, Briggs JP (1999) Expression of peroxisome proliferator-activated receptors and retinoid X receptors in the kidney. Am J Physiol 277:F966–F973

37. Yeh JI, Gulve EA, Rameh L, Birnbaum MJ (1995) The effects of wortmannin on rat skeletal muscle. J Biol Chem 270:2107–2111